

Nucleon spin structure II: Spin structure function g_1^p at small x

Wei Zhu and Jianhong Ruan

Department of Physics, East China Normal University, Shanghai 200062, P.R. China

Abstract

The spin structure function g_1^p of the proton is studied in a two component framework, where the perturbative evolution of parton distributions and nonperturbative vector meson dominance model are used. We predict the g_1^p asymmetric behavior at small x from lower Q^2 to higher Q^2 . We find that the contribution of the large gluon helicity dominates g_1^p at $x > 10^{-3}$ but mixed with nonperturbative component which complicates the asymptomatic behavior of g_1^p at $x < 10^{-3}$. The results are compatible with the data including the HERA early estimations and COMPASS new results. The predicted strong Q^2 - and x -dependence of g_1^p at $0.01 < Q^2 < 3\text{GeV}^2$ and $x < 0.1$ can be checked on the next Electron-Ion Collider.

PACS number(s): 12.38.Cy, 12.38.Qk, 12.38.Lg, 12.40.Vv

keywords: Nucleon spin structure

1 Introduction

Recently, COMPASS experiment at CERN collected a large number of events of polarized inelastic scattering off the protons with very small values of Bjorken scaling variable x [1]. The preliminary analysis of these data combining with the previous experiments [2], showed non zero and positive asymmetries of the structure function g_1^p . In these fixed target experiments the low values of x are almost reached by lowering the values of Q^2 . The knowledge of the nucleon spin structure function $g_1(x, Q^2)$ at low Q^2 and small x is particularly interesting, since it is not only an important information to resolve the "proton spin crisis", but also provides us with a good place to study the transition from the perturbative research to the nonperturbative description of the proton structure.

In this work we try to study the behavior of g_1^p at small x but in the full Q^2 range. As we know that the structure functions of the nucleon are mainly constructed of the parton distributions at $Q^2 > 1\text{GeV}^2$, while the non-perturbative contributions to the structure functions become unneglectable at $Q^2 \ll 1\text{GeV}^2$. A key question is what components construct the spin structure functions of the proton at such low Q^2 ? Particularly, do the parton distributions and their pQCD evolution still play a role or not? For answering these questions, we introduce the application of the Dokshitzer-Gribov-Lipatov-Altarelli-Parisi (DGLAP) equation [3] with the parton recombination corrections at low Q^2 in detail. These corrections have been derived both for the polarized and unpolarized parton distributions in our previous works [4,5]. We point out that the isolation of the contributions of the vector meson is necessary for keeping the factorization schema of the polarized parton distributions at low Q^2 . We find two different asymptotic behaviors of g_1^p at $x < 10^{-3}$: nonperturbative behavior $\sim x^{-1}$ at $Q^2 < 1\text{GeV}^2$ and perturbative drop at $Q^2 > 3\text{GeV}^2$. We predict the translation of g_1^p at small x from lower Q^2 to higher Q^2 . The results are compatible with the data including the early HERA estimations and COMPASS new results. We point out that the measurements at different x with different values of Q^2 in the fixed target experiments mix the complicated asymptomatic behavior of g_1^p . The predicted strong Q^2 - and x -dependence of g_1^p at $0.01 < Q^2 < 3\text{GeV}^2$ and $x < 0.1$ due to the mixture of nonperturbative vector meson interactions and the QCD evolution of the

parton distributions can be checked on the next Electron-Ion Collider (EIC).

The organization of this paper is as follows. In Sec. 2 we discuss the applications of the polarized parton distributions at low Q^2 based on the generalized leading order approximation. In Sec.3 we summarize the contributions of the polarized parton distributions to the spin structure function g_1^p of the proton, which have been fixed by our previous work. The contributions of the vector meson to g_1^p are discussed in Sec. 4. We present our predictions of g_1^p and the comparisons with the data in Sec. 5. The discussions and summary are given in Sec. 6.

2 A general consideration of the nucleon structure function at low Q^2

In the researches of the nucleon structure functions at the full kinematic region, an argued question is whether the parton distributions and their perturbative QCD evolution can (even partly) be applied to the low Q^2 range or the parton concept is suddenly invalid at a critical value of $Q^2 \leq 1\text{GeV}^2$?

Let us begin from the parton model for the spin-dependent distribution, which is written based on the Collins-Soper-Sterman (CSS) factorization schema [6] at the collinear approximation and the twist-2 level,

$$g_1(x, Q^2) = \int_0^1 \frac{dy}{y} \sum_q C_q(x/y, Q^2/\mu_F) \delta q(y, \mu_F), \quad (2.1)$$

which breaks up the spin structure function into two factors associated with perturbative short-distance functions C_a and nonperturbative polarized parton distributions δq at the factorization scale μ_F .

Taking the lowest order of C_q

$$C_q(x/y, Q^2/\mu_F) = \frac{1}{2} e_q^2 \delta(x/y - 1) \delta(Q - \mu_F) + \mathcal{O}(\alpha_s) + \mathcal{O}(1/Q), \quad (2.2)$$

$\mathcal{O}(\alpha_s)$ and $\mathcal{O}(1/Q)$ are the QCD radiative corrections and higher twist contributions. Inserting it to Eq. (2.1), we obtain the relation between the spin structure functions and the polarized quark distributions

$$g_1(x, Q^2) = \frac{1}{2} \sum_q e_q^2 [\delta q(x, Q^2) + \delta \bar{q}(x, Q^2)] + \mathcal{O}(\alpha_s) + \mathcal{O}(1/Q). \quad (2.3)$$

According to the renormalization group theory,

$$\frac{dg_1(x, Q^2)}{d \ln \mu_F} = 0, \quad (2.4)$$

it gives the DGLAP equation

$$Q^2 \frac{d}{dQ^2} \delta q(x, Q^2) = \int_0^1 \frac{dy}{y} \sum_{q'} \Delta P_{qq'}(x/y, \alpha_s(Q^2)) \delta q'(y, Q^2), \quad (2.5)$$

$\Delta P_{qq'}$ denotes the splitting functions. If we consider only the leading order (*LO*) approximation, we have

$$g_1^{DGLAP}(x, Q^2) = \frac{1}{2} \sum_q e_q^2 [\delta q(x, Q^2) + \delta \bar{q}(x, Q^2)], \quad (2.6)$$

These results are available at $Q^2 >$ a few GeV^2 .

Now let us consider what will happen to the above results at low Q^2 ? In principle, the initial parton distributions $\delta q(x, \mu^2)$ in Eq. (2.1) are defined at $Q^2 = \mu^2$ ($\Lambda_{QCD} < \mu \ll 1GeV$). Therefore, the parton distributions are non-perturbative essentially. However, the factorization in Eq.(2.1) should be modified at low Q^2 because of the following reasons:

(i) The handbag diagram Fig.1a is a typical time ordered diagram describing Eq. (2.1), where the quark propagators connecting with the probe and the target have only the forward component, these propagators can be broken as shown in Eq. (2.1) since they are on-mass-shell. The corresponding backward quark propagators construct the cat's ear diagram Fig.1b, which are neglected since these backward propagators are absorbed by the target in the collinear approximation [7]. However, the contributions of Fig. 1c to Eq. (2.1) can not be neglected at low Q^2 due to the corrections of quark-antiquark pair, which interacts with the target as a virtual vector meson if the transverse momentum $k_\perp \sim Q$ of quark pair is not large and confinement effects are essential. The interference of the forward and backward quark propagators in Fig. 1a and 1c will put these propagators to off-mass-shell and breaks the factorization schema. To avoid this event, we use a phenomenological vector meson dominance (VMD) model [8] to "isolate" the contributions from Fig. 1c. Traditionally, such VMD hypothesis is used to explain the structure function at low Q^2 region [9]. We denote this contribution as $g_1^{VMD}(x, Q^2)$.

(ii) In CSS collinear factorization scheme the soft gluons connect with the hard- and soft-parts can be absorbed into the soft-part at the collinear approximation, where the transverse momentum k_T of the partons is neglected. However, the k_T -effects of the parton

at low Q^2 should be considered. Thus, the collinear factorization should be replaced by the k_T -factorization scheme. Unfortunately, we haven't a satisfy k_T -factorization scheme for the spin structure functions. The k_T -effects also include the replacements of $\delta q(x, Q^2)$ and the DGLAP equation with the transverse momentum dependent (TMD) distribution $\delta q(x, k_T, Q^2)$ and corresponding new evolution equations. While we haven't such tools yet. We assume that a satisfactory choice of the parameters in the input parton distributions can mimic these k_T -effects.

(iii) According to the operator product expansion (OPE) in QCD [10], the Q^2 -evolution of structure function moments can be described in terms of twist expansion. The twist-2 represents the scattering from individual partons, while higher twist corrections appear due to correlations among partons. At low Q^2 scale, the higher twist (HT) contributions to the structure functions play a significant role. A special twist-4 corrections-the parton recombination to the DGLAP evolution equation at $LL(Q^2)$ approximation has been derived by us for un-polarized and polarized parton distributions in [4,5]. We will detail its contribution $g_1^{DGLAP+ZRS}$ in next section. While the typical contributions of the higher twist power suppressions $\sim \sum_{i=2}^{\infty} \mu_{2i}(x, Q^2)/Q^{2i-2}$ to g_1^p are neglected in this work since they mainly change g_1^p at $x > 0.1$ [11].

(iv) The more complicated corrections to g_1 at low Q^2 are from the higher order QCD effects $\mathcal{O}(\alpha_f)$. In our works we only consider the contributions of the leading order corrections. An unavoidable question is whether we can neglect all higher order QCD corrections when $Q^2 \ll 1GeV^2$? Since all order resummation of these corrections are difficult, we take following generalized leading order (GLO) approximation [12]: if the leading order contributions (or including necessary lowest order corrections) to a given process are compatible with the experimental data, one can conjecture that these neglected higher order corrections to this process may cancelable each other, or they are successfully absorbed by a finite number of free parameters.

In consequence, at small x and low Q^2 we have

$$g_1(x, Q^2) \simeq g_1^{DGLAP+ZRS}(x, Q^2) + g_1^{VMD}(x, Q^2), \quad (2.7)$$

We will detail every term of Eq. (2.7) in next sections.

3 Contributions of parton distributions

In this section, we present the contributions of the polarized parton distributions of the proton to the spin structure functions at low Q^2 , i.e.,

$$g_1^{DGLAP+ZRS}(x, Q^2) = \frac{1}{2} \sum_q e_q^2 [\delta q(x, Q^2) + \delta \bar{q}(x, Q^2)], \quad (8)$$

where the QCD evolution dynamics take the DGLAP equation with the parton recombination (ZRS) corrections at the $LL(Q^2)$ approximation (see Eqs. (2.1)-(2.11) in Ref.[12]), the minimum free parameters in the input parton distributions have been fixed by the data mainly at $x > 10^{-2}$, they are

$$xu_v(x, \mu^2) = 24.3x^{1.98}(1-x)^{2.06}, \quad (3.1)$$

$$xd_v(x, \mu^2) = 9.10x^{1.31}(1-x)^{3.8}, \quad (3.2)$$

in [13], and

$$\delta u_v(x, \mu^2) = 40.3x^{2.85}(1-x)^{2.15}, \quad (3.3)$$

$$\delta d_v(x, \mu^2) = -18.22x^{1.41}(1-x)^{4.0}, \quad (3.4)$$

at $\mu^2 = 0.064 GeV^2$ in [12]. The input distributions Eqs. (3.1-3.4) neglect the contributions of asymmetry sea quark corrections.

Note that $1/\mu = 0.78 fm$ consists with a typical proton scale $0.8 - 1 fm$. We consider that μ is a minimum transverse momentum of the partons in the proton due to the uncertainty principle. Thus, we assume that all parton distributions are freezed at scale Q^2 if $Q^2 \leq \mu^2$. Based on this assumption we avoid the un-physical singularities at $Q \sim \Lambda_{QCD}$.

We present x -dependence of $g_1^{DGLAP+ZRS}(x, Q^2)$ at several values of Q^2 in Fig. 2. One can find the dramatic change of the spin structure function at $x < 10^{-3}$ from a flat form

to dramatically decreasing. Considering Fig. 3 in Ref.[12], we conclude that the large gluon helicity effect leads to this phenomenon.

4 Contributions of the VMD part

As we have emphasized that the contribution from the vector meson in virtual photon to g_1^p at $Q^2 < 1\text{GeV}^2$ is necessary. Traditionally, this correction of the vector meson can be described by the VMD model and it had been used for the predictions of structure function at small x and low Q^2 region.

This contribution is written as

$$xg_1^{VMD}(x, Q^2) = \frac{m_v^2}{8\pi} \sum_v \frac{m_v^2 Q^2}{\gamma_v^2 (Q^2 + m_v^2)^2} \Delta\sigma_{vp}(s), \quad (4.1)$$

where γ_v is the coupling constant of vector meson and proton; x is a variable defined as $x = Q^2/(s + Q^2 - m_p^2)$ rather than a momentum fraction of parton, s is the CMS energy square for the γp collision. The contributions of ω meson are similar to that of ρ , while the contributions of ϕ meson are small at $Q^2 < 1\text{GeV}^2$ and can be neglected. We take $v = \rho$ and ω at $Q^2 < 1\text{GeV}^2$ and $m_v = 0.770\text{GeV}$. The cross-sections $\Delta\sigma_{vp}(s)$ is the total cross section for the scattering of polarized meson with the nucleon, unfortunately, they are unknown. Usually, the following parameterized formula is used,

$$\Delta\sigma_{vp}(s) \sim s^{\lambda-1}, \text{ at } x < x_0. \quad (4.2)$$

Thus, we take

$$g_1^{VMD}(x, Q^2) = B \frac{(m_v^2)^{2-\lambda} (Q^2)^\lambda}{(Q^2 + m_v^2)^2} \left[\left(\frac{x}{x_0}\right)^{-\lambda} \theta(x_0 - x) + \frac{\ln^4 x}{\ln^4 x_0} \theta(x - x_0) \right], \quad (4.3)$$

where the second factor at $x > x_0$ is an arbitral function to suppress the contributions of the VMD mechanism with increasing x . The extrapolation of g_1^p from the measured region down to $x \sim 0$ suggest us to assume that $\lambda = 1 - \epsilon$ and $x_0 = 10^{-3}$, where $\epsilon \sim 0$ is a small positive parameter due to the requirement of integrability of g_1^p at $x \rightarrow 0$. In this work, we temporarily take $\epsilon = 0$. Thus,

$$g_1^{VMD}(x, Q^2) = B \frac{m_v^2 Q^2}{(Q^2 + m_v^2)^2} \left[\left(\frac{x_0}{x}\right) \theta(x_0 - x) + \frac{\ln^4 x}{\ln^4 x_0} \theta(x - x_0) \right], \quad (4.4)$$

where the parameter $B = 3$.

5 Predictions for spin structure function g_1^p at small x

What is the asymptotic behavior of g_1^p ? This is a broadly discussed subject. We plot $g_1^p(x, Q^2) = g_1^{DGLAP+ZRS}(x, Q^2) + g_1^{VMD}(x, Q^2)$ with different values of Q^2 in Fig. 3. There are two different asymptotic behaviors of g_1^p at $x < 10^{-3}$: the VMD behavior $\sim x^{-1}$ at $Q^2 < 1\text{GeV}^2$ and the large gluon helicity effect at $Q^2 > 3\text{GeV}^2$. Besides, g_1^p presents the twist form of the two asymptomatic behaviors above, which is the mixing result of the nonperturbative and perturbative dynamics.

We compare our predicted g_1^p at $x > 10^{-3}$ with the data [14] in Fig. 4. These data on 2010 are more precise than the previous data. Note that the values of Q^2 of every measured point are different and they are taken from Table I of [14]. The theoretical curve is a smooth connection among these points. This figure shows that the pQCD evolution almost control the behavior of g_1^p at $x > 10^{-3}$.

On the other hand, the combination of non-perturbative and perturbative dynamics at $x < 10^{-3}$ leads to a dramatic change of g_1^p around $Q^2 = 1 \sim 3\text{GeV}^2$. Unfortunately, there are only several data with large uncertainty about g_1^p in this range. In Figs. 5 and 6 we collect the HERA early data [15,16] at $Q^2 = 1, 10\text{GeV}^2$ which are un-generally used and compare them with our predicted g_1^p . Figure 7 shows some of these data (trigon) [15] and the comparisons with our results (dark points). Figure 8 is the Q^2 -dependence of g_1^p with fixed x , the data are taken from [17]. One can find that our predicted g_1^p are compatible with these data, although more precise measurements are necessary.

Finally, we compare our results with the new COMAPSS (primary) data [1,2] at $Q^2 < 1\text{GeV}^2$, which show that g_1^p presents a flat asymptomatic form at $x < 10^{-3}$. This seems to contradict with the predicted strong rise of g_1^p at $Q^2 < 1\text{GeV}^2$ in Fig.3. However, in the COMPASS fixed target experiments there is a strong correlation between x and Q^2 , which makes low x measurements also with low Q^2 . In Fig. 9 we take the average values of Q^2 for each probing values of x (see Fig.1 in Ref.[1]). The results are acceptable. Obviously, the measurements at different x with different values of Q^2 in the fixed target

experiments mix two different asymptomatic behaviors of g_1^p .

We predict the stronger Q^2 - and x -dependence of g_1^p at $0.01 < Q^2 < 3\text{GeV}^2$ and $x < 0.1$ due to the mixtion of nonperturbative vector meson interactions and the QCD evolution of the parton distributions in Fig. 3. For testing this prediction, the measurements of g_1^p with fixed x or Q^2 at low Q^2 are necessary. The planning Electron-Ion Collider (EIC), for example, eRHIC [18] and EIC@HIAF [19] can probe a broad low $Q^2 < 1\text{GeV}^2$ -range, where we can check the predicted behavior of g_1^p at fixed x or Q^2 .

6 Discussions

In general consideration, both the logs of $1/x$ and Q^2 are equally important at small x and low Q^2 , and one should sum the double logarithmic (DL) terms $(\alpha_s \ln^2(1/x))^n$, which predict the singular behavior $g_1^p \sim x^{-\lambda}$ ($\lambda > 0$). To this end, some special attentions are proposed [20]. For example, the double logarithmic terms are taken into account via a suitable kernel of the evolution equations in the infrared evolution equations, which was first suggested by Lipatov [21], or alternatively taking a singular initial parton distributions at $x < 10^{-2}$, one can also mimic the results of the DL-resummation.

In this work, the behavior of g_1^p at the same range is obtained through a long evolution of the DGLAP equation with the parton recombination corrections. We find that it is different from the predictions of the DL-resummation, the asymptomatic behavior of the polarized quark distributions at $x \rightarrow 0$ is controlled by ΔP_{qg} in the DGLAP equation, rather than the $\ln^k(1/x)$ -corrections to the DGLAP-kernel. Thus, the difficult DL resummation can be replaced by the fits of the initial quark distributions $\delta q_v(x, \mu^2)$ in the DGLAP equation if the evolution distance is long enough. This conclusion was also obtained in the unpolarized structure functions [22].

In summary, we use the DGLAP equation with the parton recombination corrections and the nonperturbative vector meson dominance model to predict the spin structure functions g_1^p of the proton. We first present a complete picture for the translation of g_1^p from low Q^2 (~ 0) to high Q^2 at small x . We find that the contribution of the large gluon helicity dominates g_1^p at $x > 10^{-3}$, but the mixtion with nonperturbative component complicates the asymptomatic behavior of g_1^p at $x < 10^{-3}$. The results are compatible with the data including the early HERA estimations and COMPASS new results. The predicted strong Q^2 - and x -dependence of g_1^p at $0.01 < Q^2 < 3\text{GeV}^2$ and $x < 0.1$ due to the mixtion of nonperturbative vector meson interactions and the QCD evolution of the parton distributions can be checked on the next Electron-Ion Collider (EIC).

References

- [1] A.S. Nunes (on behalf of the COMPASS Collab.,) Longitudinal double spin asymmetry A_1^p and spin-dependent structure function g_1^p of the proton at low x and low Q^2 from COMPASS, Proceedings of the XV workshop on high energy spin physics, Dubna, Russia, (2013), hep-ex/1405.5811.
- [2] COMPASS Collaboration, P. Abbon et al., Nucl. Instr. and Meth. **A577**, 455 (2007); E.S. Ageev et al., Phys. Lett. **B612**, 154 (2005); V.Yu. Alexakhin et al., Phys. Lett. **B647**, 8 (2007); M.G. Alekseev et al., Phys. Lett. **B690**, 466 (2010).
- [3] G. Altarelli, G. Parisi, Nucl. Phys. **B126**, 298 (1977); V.N. Gribov, L.N. Lipatov, Sov. J. Nucl. Phys. **15**, 438 (1972); Yu.L. Dokshitzer, Sov. Phys. JETP **46**, 641 (1977).
- [4] W. Zhu, Nucl. Phys. **B551**, 245 (1999), hep-ph/9809391; W. Zhu, J.H. Ruan, Nucl. Phys. **B559**, 378 (1999), hep-ph/9907330v2; W. Zhu and Z.Q. Shen, HEP & NP, **29**, 109 (2005), hep-ph/0406213v3.
- [5] W. Zhu, Z.Q. Shen and J.H. Ruan, Nucl. Phys. **B692**, 417 (2004), hep-ph/0406212v2.
- [6] J.C. Collins, D.E. Soper, G. Sterman, in: A.H. Mueller (Ed.), Perturbative Quantum Chromodynamics, World Scientific, Singapore, 1989, p. 1.
- [7] W. Zhu, H.W. Xiong, J.H. Ruan, Phys. Rev. **D60**, 094006 (1999); W. Zhu, Nucl. Phys. **A753**, 206 (2005).
- [8] J.J. Sakurai, currents and mesons, university of Chicago, Chicago (1969); T. H. Bauer et al., Rev. Mod. Phys. **50**, 261 (1978); G. Grammer Jr and J. D. Sullivan, in Electromagnetic Interactions of Hadrons, edited by A. Donnachie and G. Shaw, Plenum, New York, 1978, Vol.2.
- [9] B. Badelek, J. Kwieciski, B. Ziaja, Eur. Phys. J. **C26**, 45 (2002); Acta Phys. Polon. **B33**, 3701 (2002).

- [10] G. Sterman, An Introduction to Quantum Field Theory, Cambridge Univ. Press, Cambridge, 1993.
- [11] E. Leader, A. V. Sidorov, D. B. Stamenov, the proceedings of First Workshop on Quark-Hadron Duality and the Transition to pQCD, Frascati, June 6-8, 2005, hep-ph/0509183.
- [12] W. Zhu and J.H. Ruan, Nucleon spin structure I: a dynamical determination of polarized gluon distribution in the proton, this serious works.
- [13] X.R. Chen, J.H. Ruan, R. Wang, P.M. Zhang and W. Zhu, Int. J. Mod. Phys. **E23**, 1450057 (2014), hep-ph/1306.1872; ibid **E23**, 1450058 (2014), hep-ph/1306.1874.
- [14] COMPASS Collaboration, M.G. Alekseev, et al Phys. Lett. **B690**, 466 (2010).
- [15] R. D. Ball, A. Deshpande, S. Forte, V. W. Hughes, J. Lichtenstadt,, G. Ridolf, Measurement of the polarized structure function $g_1^p(x, Q^2)$ at HERA, hep-ph/9609515.
- [16] J. Kwiecinski and B. Ziaja, hep-ph/9802386.
- [17] A. De Roeck, A. Deshpande, V.W. Hughes, J. Lichtenstadt, G. Radcl Eur. Phys. J. **C6**, 121 (1999).
- [18] E.C. Aschenauer, et. al., eRHIC Design Study: An Electron-Ion Collider at BNL, hep-ph/1409.1633.
- [19] X.R. Chen, An Electro Ion Collider Plan in China, Invited talk at the 21st International Symposium on Spin Physics, Beijing, China, Oct. 20-24 (2014).
- [20] D. Kotlorz and A. Kotlorz, Acta Phys. Polon. **B39**, 1913 (2008); B.I. Ermolaev, M. Greco, S.I. Troyan, Riv. Nuovo Cim. **33**, 57 (2010).
- [21] L.N. Lipatov. Zh.Eksp.Teor.Fiz. **82**, 991 (1982); Phys. Lett. **B116**, 411 (1982).
- [22] M. Glück, E. Reya, and A. Vogt, Eur. Phys. J. **C5**, 461 (1998).

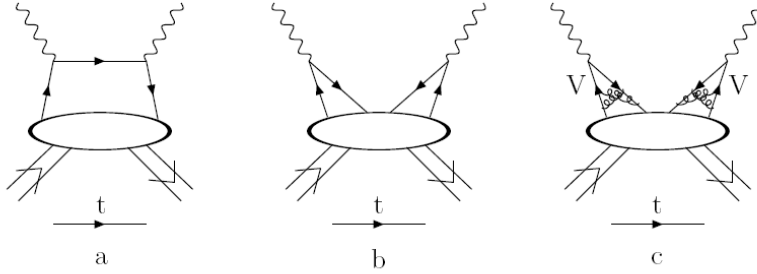


Figure 1: The time ordered decomposing of DIS diagrams. (a) The struck quarks are on-mass-shell since they have only forward component. (b) A "cat ear" diagram, which vanishes in the collinear factorization schema. (c) The "cat ear" diagram with higher order QCD corrections, which are non-vanished at low Q^2 , but can be isolated using a naive VMD model.

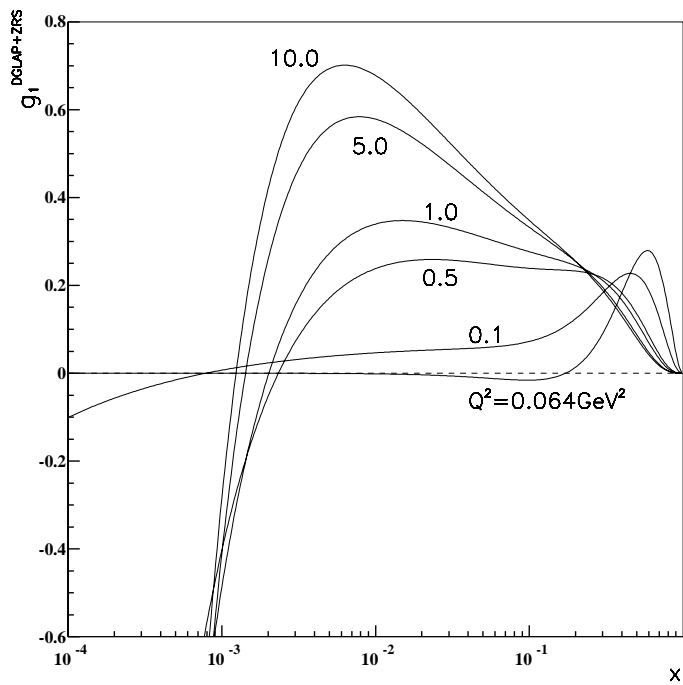


Figure 2: Perturbative contributions $g_1^{DGLAP+ZRS}$ to g_1^p . All partons are evolved from three valence quarks at $\mu^2 = 0.064 \text{ GeV}^2$.

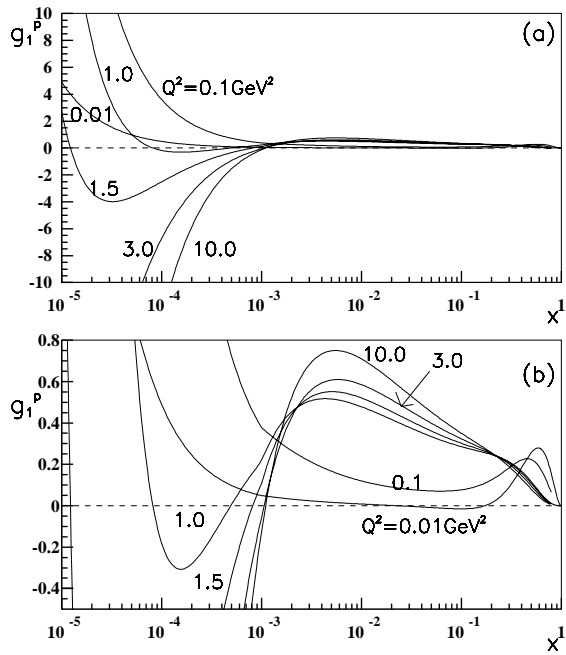


Figure 3: g_1^p evolutions at different values of Q^2 in (a) large and (b) small scales.

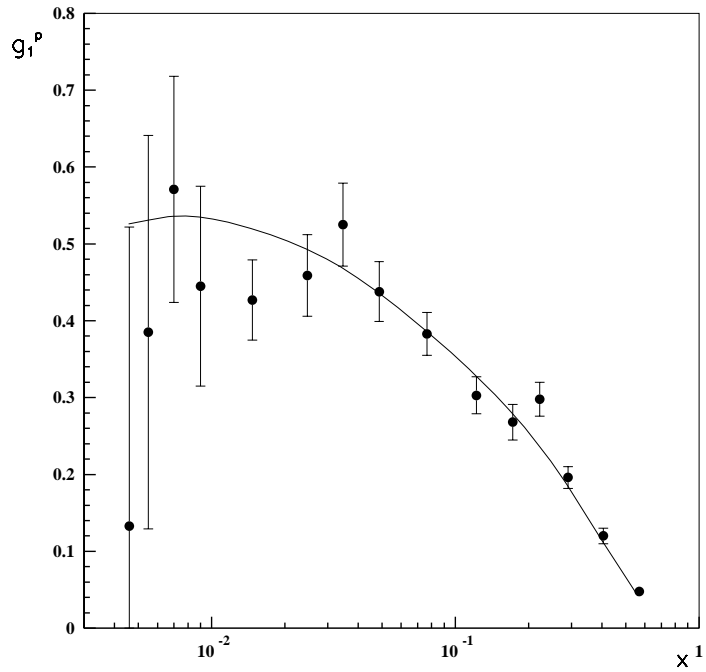


Figure 4: Predicted g_1^p at $x > 10^{-3}$ and comparisons with the COMPASS data [14]. Note that the values of $Q^2(x)$ of each measured point are different (see Table I of Ref.[14]).

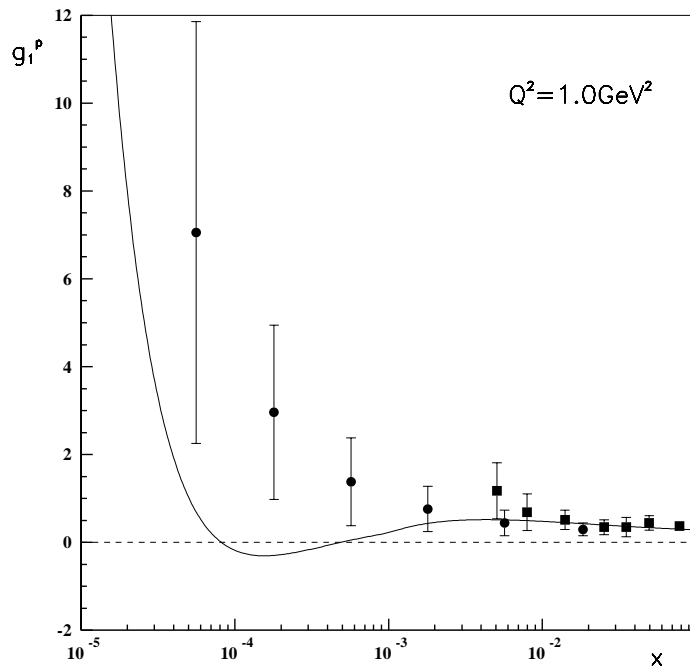


Figure 5: Predicted g_1^p at $Q^2 = 1 \text{ GeV}^2$ and the comparison with the HERA data [15].

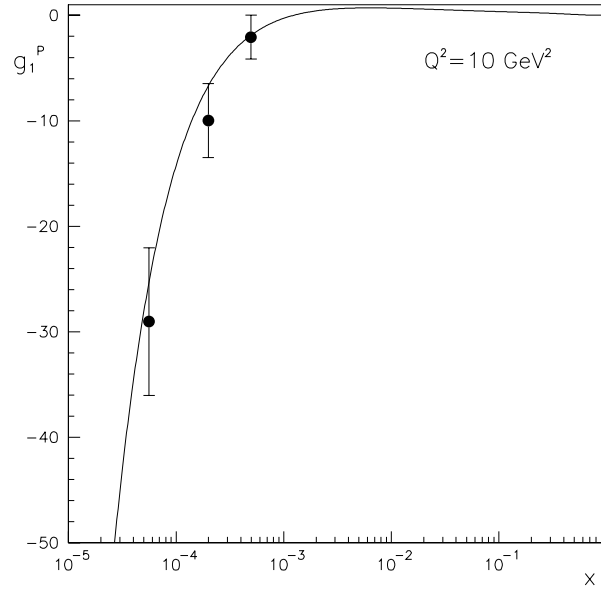


Figure 6: Predicted g_1^p at $Q^2 = 10\text{GeV}^2$ and the comparison with the HERA "data", which are based on the NLO QCD predictions with the statistical errors expected at HERA [16].

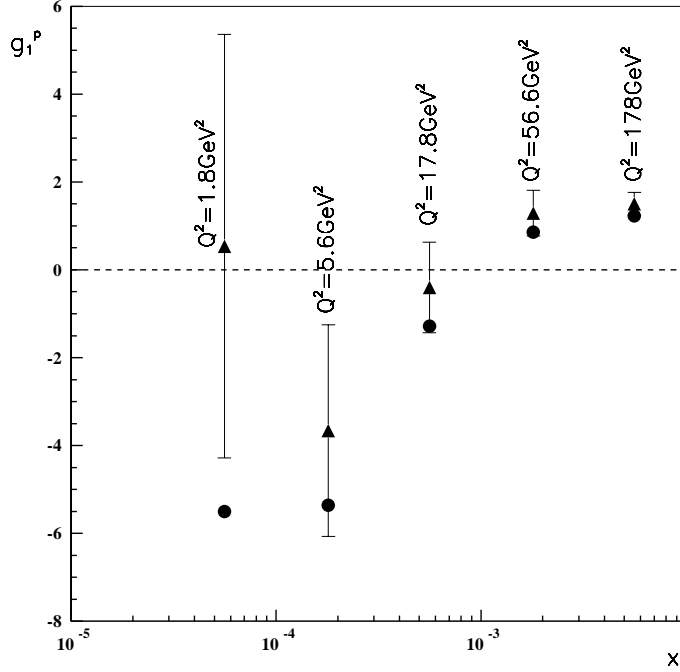


Figure 7: Predicted g_1^p at $Q^2 = 1.8\text{GeV}^2$, 5.6GeV^2 and 16.5GeV^2 at $x < 10^{-3}$ (circles) and the comparison with the HERA data (triangles) [15].

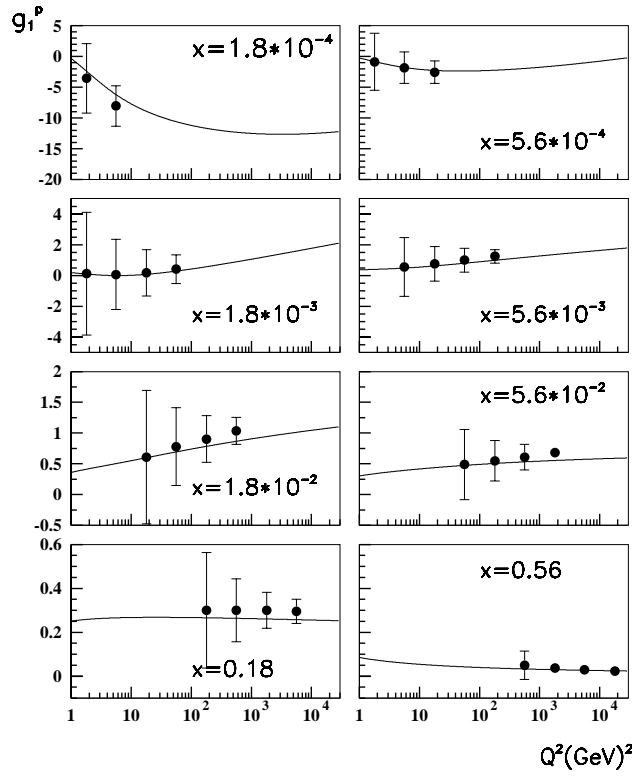


Figure 8: Predicted Q^2 -dependence of g_1^p with fixed values of x . Data are taken from [17].

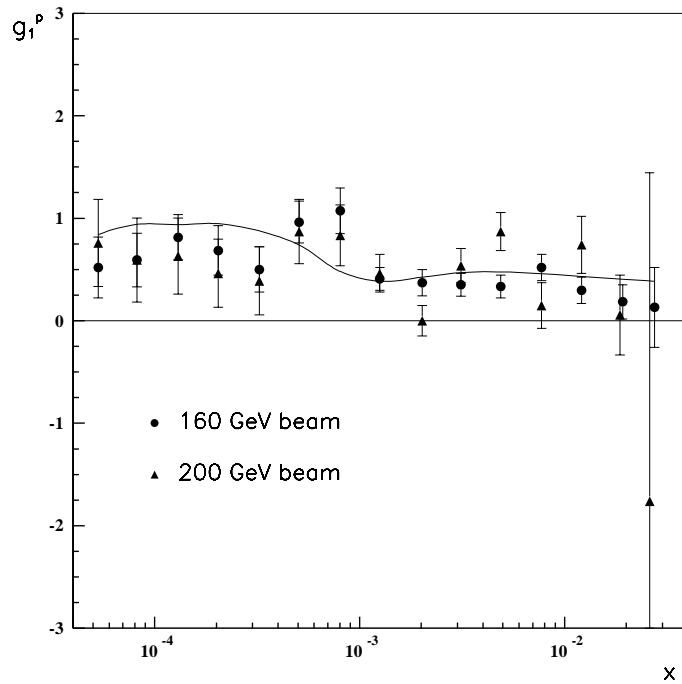


Figure 9: Predicted g_1^p as a function of x with different measured $Q^2(x)$ (solid curve). Note that the low values of x connect with the low values of $Q^2(x)$. The data are taken from COMPASS primary results with two different beam energies [1].